



Three-component Pomeron model in high energy pp - and $\bar{p}p$ - elastic scattering

A. Lengyel, Z. Tarics

Institute of Electron Physics, Ukrainian Nat. Ac. of Sci.
Universitetska, 21, Uzhgorod, Ukraine

We assume that the Pomeron is a sum of Regge multipoles, each corresponding to a finite gluon ladder. From the fit to the data of pp - and $\bar{p}p$ - scattering at high energy and all available momentum transfer we found that taking into account the spin, three-term multipole Pomeron and Odderon with different form-factors are substantial for good description of differential, total cross section and ratio ρ in the whole high energy experimental domain.

1. Introduction

The Pomeron being an infinite gluon ladder ¹⁻⁴ may appear as a finite sum of gluon ladders corresponding to a finite sum of Regge multipoles with increasing multiplicities ⁵⁻⁷. The first term in $\ln s$ series contributes to the total cross-section with a constant term and can be associated with a simple pole, the second one (double pole) goes as $\ln s$, the third one (triple pole) as $\ln^2 s$, etc. All Pomeron poles have unit intercept. Previously the multipole Pomeron and many-Pomerons approaches were investigated on different applications ⁸⁻¹¹ (see also review ¹²). Due to the recent experiments on elastic and inelastic proton-proton scattering by the TOTEM Collaboration at the LHC ¹³, data in a wide range, from lowest up to TeV energies, both for proton-proton and antiproton-proton scattering in a wide span of transferred momenta are now available. The experiments at TeV energies give a chance to verify different Pomeron and Odderon models because the secondary Reggeon contributions at these energies are small. Note that none of the existing models of elastic scattering was able to predict the value of the differential cross section beyond the first cone, as clearly seen in Fig.4 of the TOTEM paper ^{13,14}. This problem is still remains actual and inspired some people to construct the new and revitalize a well-known old fashioned models. Consequently for this time it is necessary to revise our concept on exchange mechanism in this distant

region of energies¹⁵⁻¹⁸. A number of models have been refined and developed¹⁹⁻²². In fact, several of used Pomeron models, as a rule, have intercept > 1 which requires the unitarisation²³, other ones have complicated structure and the overall number of parameters was fairly high^{24,25}.

Here we suggest the three-component Pomeron model inspired by the finite sum of gluon ladders extended to the whole range of available momentum transfer of high-energy pp - and $\bar{p}p$ - elastic scattering and performed a simultaneous fit to the σ_{tot} , ρ and $d\sigma/dt$ data. Our goal is to investigate the capabilities of Pomeron model as a finite sum of gluon rungs ($\ln s$ power) equivalent to single pole + dipole + tripole Pomeron with sufficiently account the spin influence and non-linear trajectory for pp - and $\bar{p}p$ - scattering in first and second diffraction cone. Our strategy is two fold: one to select a core set of experimental data, as well as models of reference, most appropriately describing the details of this basic set. First we take the set²⁶, and then - the paper²⁵.

This paper is organized as follows. In the next section, one introduces the main formulas and features of the model. In Sec. 3, we perform the comparison with experiment. In the last section, the conclusions are drawn up.

2. The model

The reduced form of nucleon-nucleon amplitude without double spin-flip accounting is²⁷:

$$A(s, t) = A_{00}(s, t) + \frac{\sqrt{-t}}{2m_p} A_{01}(s, t), \quad (1)$$

where $A_{00}(s, t)$ is spin-nonflip component and $A_{01}(s, t)$ is spin-flip component of scattering amplitude.

Our ansatz for the spin-nonflip scattering amplitude component $A_{00}(s, t)$ is:

$$A_{00}(s, t) = P_{00}(s, t) + R_f(s, t) \pm [R_\omega(s, t) + O(s, t)] \quad (2)$$

for $\bar{p}p$ (upper symbol) and pp (lower symbol) scattering respectively. For the spin-flip scattering amplitude component $A_{01}(s, t)$

$$A_{01} = P_{01}(s, t) + R_f(s, t) \pm [R_\omega(s, t) + g_{od}O(s, t)]. \quad (3)$$

We suppose that the contribution of the subleading reggeons to the spin-flip amplitude is the same as to the spin-nonflip amplitude and the contribution of Odderon to the spin-flip amplitude differ from one to the spin-nonflip amplitude by the factor g_{od} , where the Pomeron contribution we introduce in form:

$$P_{00}(s, t) = is \left(-i \frac{s}{s_0} \right)^{\alpha_P(t)-1} \sum_{j=0}^2 a_{0j} \ln^j \left(-i \frac{s}{s_0} \right) e^{\varphi_{0j}(t)} \quad (4)$$

and

$$P_{01}(s, t) = is \left(-i \frac{s}{s_0} \right)^{\alpha_P(t)-1} \sum_{j=0}^2 g_{1j} \ln^j \left(-i \frac{s}{s_0} \right) e^{\varphi_{1j}(t)}. \quad (5)$$

The Pomeron trajectory is:

$$\alpha_P(t) = 1 + \alpha'_P t + \alpha''_P (\sqrt{t_\pi} - \sqrt{t_\pi - t}), \quad (6)$$

where the lowest two-pion threshold $t_\pi = 4m_\pi^2$. The residue functions are:

$$\varphi_{0j}(t) = \gamma_{0j} (\sqrt{t_\pi} - \sqrt{t_\pi - t}), \quad (7)$$

$$\varphi_{1j}(t) = \gamma_{1j} (\sqrt{t_\pi} - \sqrt{t_\pi - t}). \quad (8)$$

In (2),(3) the $R_f(s, t)$, $R_\omega(s, t)$ and $O(s, t)$ contain the subleading reggeons as well as the Odderon contributions to the scattering amplitude:

$$R_f(s, t) = g_f \left(-i \frac{s}{s_0} \right)^{\alpha_f(t)} e^{b_f t} \quad (9)$$

and

$$R_\omega(s, t) = i g_\omega \left(-i \frac{s}{s_0} \right)^{\alpha_\omega(t)} e^{b_\omega t}, \quad (10)$$

where

$$\alpha_j(t) = 1 + \alpha'_j t, \quad j = f, \omega; \quad s_0 = 1 \text{ GeV}^2. \quad (11)$$

To describe the different behavior of proton-proton and antiproton-proton differential cross-section in region of dip-bump one needs to include the Odderon contribution, which we use in a simple form:

$$O(s, t) = s \left(-i \frac{s}{s_0} \right)^{\alpha_O(t)-1} \sum_{j=0}^2 g_j \ln^j \left(-i \frac{s}{s_0} \right) e^{\phi_j(t)}. \quad (12)$$

The Odderon trajectory is

$$\alpha_O(t) = 1 + \alpha'_O t. \quad (13)$$

The residue functions are:

$$\phi_j(t) = \delta_j \left(\sqrt{t'_\pi} - \sqrt{t'_\pi - t} \right), \quad (14)$$

$$t'_\pi = 9m_\pi^2.$$

Table 1. Parameters, quality of the fit obtained in the whole interval in s and t .

Parameter	Value	Error
a_{00}	8.449	0.121
a_{01}	-0.855	0.0188
a_{02}	0.06519	$0.81 \cdot 10^{-2}$
a_{10}	-0.3690	0.0250
a_{11}	6.134	0.0910
a_{12}	-0.1938	0.00461
α_P', GeV^{-1}	0.04638	$0.523 \cdot 10^{-2}$
γ_{00}, GeV^{-1}	2.107	0.037
γ_{01}, GeV^{-1}	0.5742	0.0562
γ_{02}, GeV^{-1}	1.422	0.0633
γ_{10}, GeV^{-1}	2.623	0.0515
γ_{11}, GeV^{-1}	6.540	0.02655
γ_{12}, GeV^{-1}	5.176	0.0354
g_{00}	-0.4855	0.0188
g_{01}	-0.4855	0.0188
g_{02}	0.06519	$0.81 \cdot 10^{-3}$
α_O', GeV^{-2}	0.05197	$0.117 \cdot 10^{-2}$
δ_0, GeV^{-1}	2.623	0.0515
δ_1, GeV^{-1}	6.450	0.026
δ_2, GeV^{-1}	5.176	0.035
g_{od}	553.6	47.7
a_f	-10.75	0.75
α_f	0.5395	0.0185
a_ω	10.17	0.44
α_ω	0.4182	0.0131
χ^2/dof	1.56	

3. Comparison with experiment

In order to determine the parameters that control the s -dependence of $A(s, 0)$ we applied a wide energy range $5GeV \leq \sqrt{s} \leq 7000GeV$ and used the available data for total cross sections and ρ (²⁶). A total of 107 experimental points were included for $t = 0$. For the differential cross sections we selected the data at the energies $\sqrt{s} = 19; 23; 31; 44; 53; 62; 7000GeV$ (for pp -scattering)(1633 experimental points) and $\sqrt{s}=31;53;62;546;1800GeV$ (510 experimental points) for $\bar{p}p$ - scattering ²⁶. The squared 4-momentum covers entire available range $0.01(GeV)^2 < |t| < 14(GeV)^2$. The grand total number of 2384 experimental points were used in overall fit. In the calculations we use the following normalization for the dimensionless amplitude:

$$\sigma_{tot} = \frac{4\pi}{s} ImA(s, t = 0), \quad (15)$$

$$\frac{d\sigma}{dt} = \frac{\pi}{s^2} [|A_{00}(s, t)|^2 - \frac{t}{4m_p^2} |A_{01}(s, t)|^2]. \quad (16)$$

The resulting fits for σ_{tot} , ρ , $\frac{d\sigma}{dt}$ are shown in Figs. 1. - 2. with the values of the fitted parameters quoted in Table 1. From these figures we conclude that the multipole Pomeron model corresponding to a sum of gluon ladders up to two rungs complicated with Odderon contribution and spin counting fits the data well in a wide energy and momentum transfer regions. In this paper, we have explored only the simplest phenomenological tripole Pomeron. In fact, the scattering amplitude is much more complicated than just a simple power series in $\ln s$. On the one hand, although we used just a simplified t -dependence in the model, reasonably good results were obtained. Because the slopes of secondary reggeons do not influence the fit sufficiently, we have fixed them at $\alpha'_f = 0.84(GeV)^{-2}$ and $\alpha'_\omega = 0.93(GeV)^{-2}$, which correspond to the values of Chew-Frautschi plot, as well as its slope parameters $b_f = 12.0(GeV)^{-2}$ and $b_\omega = 14.0(GeV)^{-2}$. Additionally we fixed the Pomeron trajectory slope $\alpha'_P = 0.4(GeV)^{-2}$. On the other hand, we included the curvature of the Pomeron trajectory that cannot be negligible. The quality of our fits $\chi^2/dof=1.56$ is comparable with that of the best fit of ²⁵.

4. Summary

We have approved the tripole Pomeron model having each term corresponding to a finite gluon ladder.

This corresponds to the finite sum of gluon ladders with up to two rungs or alternatively up to the tripole Pomeron contribution. We have obtained very good description of pp and $\bar{p}p$ hadron scattering data at intermediate and high energies and all available momentum transfer. We conclude that the nonfactorisable form of the Pomeron and Odderon amplitudes as well as the nonlinearity of its trajectory and the residue function is strongly suggested by data at all available momentum transfer. It should be noted that the addition of spin-flip component of scattering amplitude decisively improves the result of the fit.

Acknowledgments

We are grateful to L.Jenkovszky and E.Martynov for valuable suggestions and A.M.Lapidus for fruitful discussions.

Bibliography

1. E.A.Kuraev, L.N.Lipatov, V.S.Fadin, Zh. Eksp. Teor. Fiz. **72**, 377 (1977) [Sov. Phys. JETP **45**, 199 (1977)].
2. Ya.Ya.Balitsky, L.N.Lipatov, Sov. J. Nucl. Phys. **28**, 822 (1978).
3. L.N.Lipatov, Zh. Eksp. Teor. Fiz. **90**, 1536 (1986) [Sov. Phys. JETP **63**, 904 (1986)].
4. V.S.Fadin, L.N.Lipatov, Phys. Lett. **B429**, 127 (1998) and references therein.

5. R.Fiore, L.L.Jenkovszky, E.A.Kuraev, A.I.Lengyel, F.Paccanoni and A.Papa, Phys. Rev. **D63**, 056010 (2001).
6. R.Fiore, L.Jenkovszky, E.Kuraev, A.Lengyel, F.Paccanoni and Z.Tarics, Phys. Rev. **D81**, 056001 (2010).
7. A.Lengyel, Z.Tarics, Ukr. J. Phys. **58** 703 (2013).
8. P.Desgrolard, M.Giffon, E.Predazzi, Z.Phys. **C63** 241 (1994).
9. Yu.IIjin, A.Lengyel and Z.Tarics, Diffraction 2002, ed. R.Fiore et al. 109 (2002).
10. V.A.Petrov, A.V.Prokudin, Eur. Phys. J. **C23** 135 (2002).
11. K.J.Kontros, A.I.Lengyel, Z.Z.Tarics, Ukr. J.Phys. **47** 813 (2002); arXiv: 0011398v2 [hep-ph] (2001).
12. I.M. Dremin, Uspekhi Fizicheskikh Nauk **56** 3 (2013).
13. TOTEM Collaboration G.Antchev, P.Aspell, I.Atanassov, V.Avati, J.Baechler, V.Berardi, M.Berretti et al, Europhys. Lett **95** 41001 (2011).
14. TOTEM Collaboration G.Antchev, P.Aspell, I.Atanassov, V.Avati, J.Baechler, V.Berardi, M.Berretti et al, Europhys. Lett **101** 21002 (2013).
15. A.Donnachie and P.V. Landspoff, arXiv: 1309.1292 [hep-ph] (2013).
16. S.M.Troshin, N.E.Tyurin, Phys. Rev. **D88** 077502 (2013).
17. L.Frankfurt, M.Strikman, arXiv: 1304.4308v1 [hep-ph] (2013).
18. A.A.Godizov, arXiv: 1203.6013v3 [hep-ph] (2012).
19. L.L.Jenkovszky, A.I.Lengyel, D.I.Lontkovskyi, Int. J. Mod. Phys. **A 26** 4755 (2011).
20. A.I.Lengyel and Z.Z.Tarics, arXiv:1206.5837 [hep-ph](2012).
21. Jan Kaspar, Vojtech Kundrat, Milos Lokajicek, arXiv:0912.1185 [hep-ph] (2009).
22. D.A. Fagundes, G.Pancheri, A.Grau, arXiv: 1306.0452v1 [hep-ph] (2013).
23. V.A.Petrov, A.Prokudin, arXiv: 1212.1924v1 [hep-ph] (2013).
24. M.J.Menon, P.V.R.G.Silva, arXiv: 1305.2947 [hep-ph] (2013).
25. E.Martynov, Phys. Rev. **D87**, 114018 (2013).
26. File _____ with _____ the data "alldata-2.zip" is available at the address: <http://www.theo.phys.ulg.ac.be/alldata-v2.zip>.
27. K.G.Boreskov, A.M.Lapidus, S.T.Sukhorukov, K.A.Ter-Martirosyan, Yad. Fiz.**14** 814 (1971).

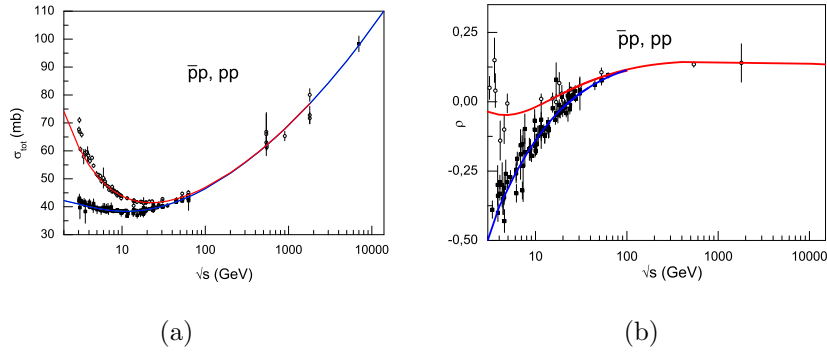


Figure 1. (a) pp and $\bar{p}p$ total cross sections calculated from the model and fitted to the data in range $\sqrt{s} = 5 \text{ GeV} - 7 \text{ TeV}$. (b) Ratio of the real to imaginary part for pp and $\bar{p}p$ scattering amplitude calculated from the same model. Upper curve - presents the $\bar{p}p$ calculation, lower curve - present pp one.

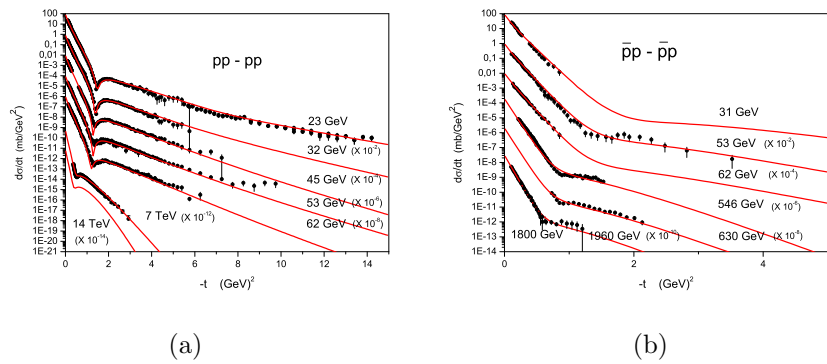


Figure 2. (a) Differential pp (a) and $\bar{p}p$ (b) cross sections calculated from the model taking into account the spin and fitted to the data in the range $-t = 0.1 - 15 \text{ GeV}^2$.